Jingxian Yu, John R. Horsley, and Andrew D. Abell

Peptides as bio-inspired electronic materials: an electrochemical and first-principles perspective

Accounts of Chemical Research, 2018; 51(9):2237-2246

Peptides as bio-inspired electronic materials: An electrochemical and first principles perspective

Jingxian Yu, John R. Horsley and Andrew D. Abell**

ARC Centre of Excellence for Nanoscale BioPhotonics (CNBP), Department of Chemistry, The University of Adelaide, Adelaide, SA 5005, Australia.

CONSPECTUS

Molecular electronics is at the forefront of interdisciplinary research, providing a major extension of the capabilities of conventional silicon-based technology, as well as providing a possible stand-alone alternative. Bio-inspired molecular electronics is a particularly intriguing paradigm, as charge transfer in proteins/peptides, for example, plays a crucial role in energy storage and conversion processes in all living organisms. However, the structure and conformation of even the simplest protein is extremely complex, and as such, model synthetic peptides containing well-defined geometry and pre-determined functionality, present as ideal platforms to mimic nature for the elucidation of fundamental biological processes, while also advancing the design and development of single-peptide electronic components.

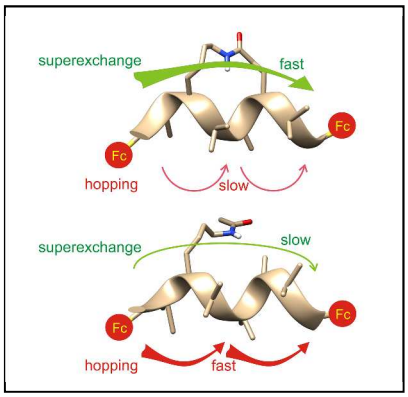

In this Account, we firstly investigate intramolecular electron transfer within two synthetic peptides, one with a well-defined helical conformation and the other a random geometry, using electrochemical techniques and constrained density functional theory (cDFT) simulations. This study reveals two definitive electron transfer pathways (mechanisms), the nature of which is dependent on secondary structure. Following on from this, electron transfer within a series of well-defined helical peptides, constrained by either Huisgen cycloaddition, ring-closing metathesis or lactam-bridge, was determined. Electrochemical results indicate that each constrained peptide, in contrast to a linear counterpart, exhibits remarkable positive formal potential shifts (> 460 mV) and significant electron transfer rate constant drops (up to 15-fold), which represent two distinct electronic 'on/off' states. High-level cDFT calculations demonstrate that the additional backbone rigidity imparted by the side-bridge constraints leads to an increased reorganization energy barrier, which restricts the torsional motions necessary for facile intramolecular electron transfer along the backbone. Moreover, cDFT calculations uncover a clear mechanistic transition from hopping to superexchange, stemming from side-bridge gating. We then extended our research to fine-tune the electronic properties of peptides through both structural and chemical manipulation, to reveal an interplay between backbone rigidity and electron-rich side-chains on electron transfer. Further to this, we explored the possibility that the side-bridge constraints present in our synthetic peptides could provide an additional electronic transport pathway, which led to the discovery of two distinct forms of quantum interferometers. The effects of destructive quantum interference occur essentially through the backbone and the additional tunnelling pathway provided by the side-bridge in the constrained β-strand peptide, as evidenced by a correlation between electrochemical measurements and molecular junction conductance (NEGF-DFT) simulations for both linear and constrained β-strand peptides. In contrast, an interplay between quantum interference effects and vibrational fluctuations is revealed in the linear and constrained helical peptides.

Collectively, these exciting findings not only augment our fundamental knowledge of charge transfer dynamics and kinetics in peptides, but also open up new avenues to design and develop functional bio-inspired electronic devices, such as on/off switches and quantum interferometers, for practical applications in molecular electronics.

1. INTRODUCTION

Electron transfer occurs in proteins over surprisingly long molecular distances of up to 100 Å to facilitate a number of crucial biological processes, including respiration and photosynthesis.[1] A fundamental understanding of electron transfer in proteins is not only central to the elucidation of these essential biological processes in living organisms, but also to the design and development of bio-inspired molecular electronic components.[2] However, the vast complexity of such systems is somewhat limiting to progress, with model synthetic peptides presenting as ideal candidates in this context. Such peptides can be designed to conform to specific secondary structures, such as helices and β-strands, to allow the dynamics and kinetics of electron transfer to be studied in a more controlled environment.[3,4] In addition, they can be specifically functionalized along their backbone to enable precision-branching, analogous to three-dimensional molecular circuitry.[5] While molecular electronics provides an opportunity to begin to redefine integrated circuit technologies,[6] one must first understand and subsequently be able to predict and control the associated charge transfer dynamics and mechanisms before this vision can be realized.

A wide variety of experimental techniques is available to investigate electron transference in peptides. Generally, these methods can be classified into three categories: (1) An extended electrode-molecule-electrode junction with a single molecule, or ensemble of molecules. This includes single-molecule STM-BJ/MCBJ conductance measurements reflected in the work by Tao,[7] Kimura,[8] & Nichols;[9] solid-state conductance measurements (Cahen[2] & Whitesides[10]) and conductive AFM characterizations (Sek[11] & Ashkenasy[3]) for an ensemble of molecules. (2) A donor-bridge-acceptor molecule for photo-induced or electrochemically-induced intramolecular electron transfer in solution, with pioneering work by Isied,[12] Giese[13] and Maran.[14] (3) An electrode-supported monolayer of peptides comprising a redox active probe for electrochemical measurements. This is a

particularly versatile technique adopted by a broader research community (Kimura[1], Kraatz[15] and our group[16]). In the literature, the terminology referred to in the first instance is "electronic transport", while in the latter two it is commonly referred to as "electron transfer".

Two distinct mechanisms are widely accepted to explain the observed dependence of electron transference on distance in peptides, namely superexchange (tunnelling) and thermally activated hopping.[12,17] The superexchange mechanism involves direct molecule-mediated tunnelling, where the intervening peptide chain has a virtual role. In this one-step process, the electron transfer rate constant (or conductance) decreases exponentially with increasing distance between the donor and acceptor (or the two electrodes).[18] The alternative hopping mechanism operates by using sites on the peptide chain that are coupled to each other electronically for electron transference, resulting in shorter and therefore faster sequential steps. In this multi-step process, electrons reside on the peptide chain for a finite time, with molecular conductance obeying ohmic behaviour with increasing distance between donor and acceptor, enabling efficient long-range electron transfer.[13]

Apart from chain length, several other factors influence electron transfer kinetics in peptides, such as the extent of secondary structure, dipole orientation, the specific component amino acids, and hydrogen bonding. A number of comprehensive reviews have discussed the influence of these factors,[19,20] some with specific emphasis on electron transfer through electrode-supported monolayers,[15] nanoscale molecular junctions,[11] and solid-state electronic transport.[2] This article focuses mainly on our recent novel findings on the relationship between electron transfer dynamics and kinetics, including the influence of secondary structure, backbone rigidity, and controllable mechanistic transition of charge transfer, from an electrochemical and first principles perspective. We also discuss the correlation between electron transfer and electronic transport, including the role of quantum interference in peptides.

2. ELECTRON TRANSFER DYNAMICS: SUPEREXCHANGE VS HOPPING

To gain insights into electron transfer dynamics, two β-peptides (**1** and **2**, see Figure 1) were synthesized by our group for electrochemical study.[21] β-Peptides are used as they are known to adopt stable helical secondary structures with high predictability.[22,23] Here, an *N*-terminal *tert*-butyl hydroperoxide is used as the electron acceptor, and *C*-terminal *p*-cyanobenzamide as the donor. Circular dichroism and NMR analysis reveals that the backbone of **2** folds into a 3_{14}-helical structure, which is consistent with geometry optimization[21,24] using the density functional theory (DFT) method. Calculations for **1** suggest that it adopts an ill-defined conformation. A series of cyclic voltammograms was obtained for both peptides on glassy carbon electrodes in 0.1 mol L^{-1} $TBAPF_6$ / DMF solutions (see Figure 1).

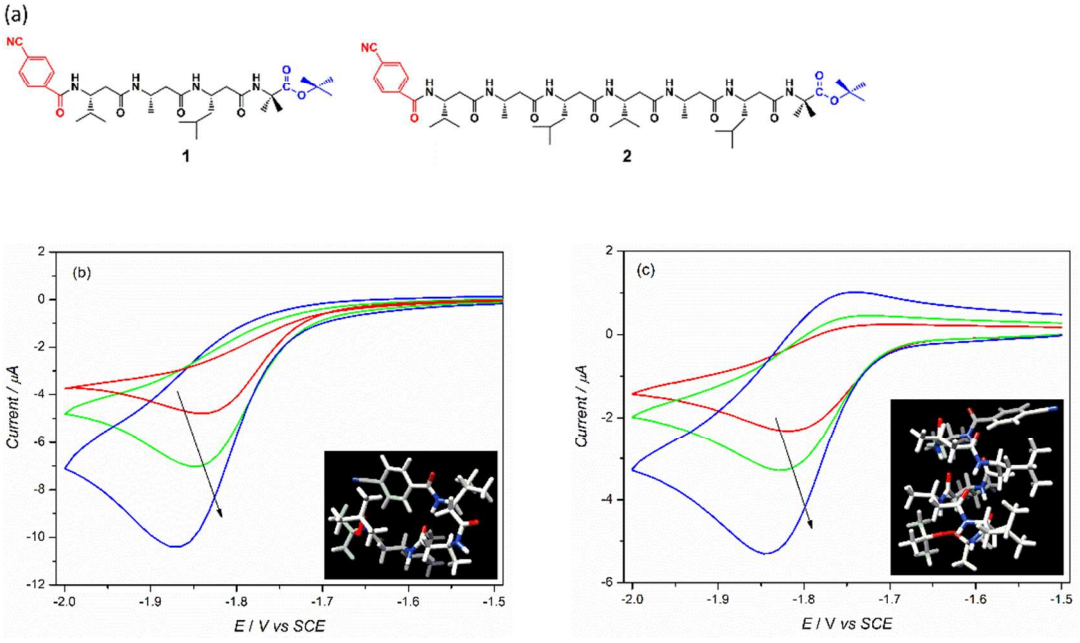

Figure 1. (a) Synthetic peptides **1** and **2**. (b) Cyclic voltammograms of **1** and (c) **2** with scan rates of 100, 200 and 500 mV s^{-1} respectively, as indicated by the arrow from top to bottom. Insets: Lowest energy conformer of each peptide.

Intramolecular electron transfer rate constants (k_{ET}), estimated by fitting the cyclic voltammograms to the dissociative electron transfer mechanism,[14] were found to decrease from 2580 s^{-1} (**1**) to 9.8 s^{-1} (**2**), nearly three orders of magnitude. According to Marcus theory,[25] k_{ET} depends exponentially on the distance for a superexchange electron transfer reaction,

$$k_{ET} = A \cdot e^{-\beta \cdot r_{DA}}$$

where r_{DA} is the distance between donor and acceptor, A is a pre-exponential factor, and β the distance decay parameter. Our DFT calculations reveal the r_{DA} as 7.57 Å for **1**, and 9.97 Å for **2**. β values can vary between 0.84-1.4 $Å^{-1}$ for peptides.[13,19] With the steepest distance decay of 1.4 $Å^{-1}$, the difference between r_{DA} of **1** and **2** should give a k_{ET} ratio of 28:1. The remarkable disparity between the measured k_{ET} for these two peptides (more than two orders of magnitude) implies that the mechanism of electron transfer in these peptides is defined by the extent of secondary structure, rather than simply by chain length. Thus, a donor-bridge-acceptor theoretical framework composed of *N*-bridging units[26] was adopted to provide further insights into electron transfer dynamics and to identify the appropriate electron transfer pathways.

For this, Marcus theory was used in combination with the latest constrained density functional theory (cDFT) to model the diabatic states in both peptides. The diabatic states in **1** and **2** were obtained by individually localizing an overall charge of -1 on the donor (D), each of the amino acids, and the acceptor (A). Figure 2 shows constructed diabatic states for both peptides and the two possible electron transfer pathways, namely superexchange and sequential hopping. For **1**, the electron transfer rate constants for the forward steps D→B1, B3→A, and backward step A→B3 along the peptide backbone are extremely small, indicating a highly improbable electron transfer route. This is consistent with a superexchange pathway in this peptide. In contrast, the electron transfer rate constants for the forward (D→A) and backward (A→D) steps for peptide **2** are

exceptionally small. This implies that a superexchange mechanism does not occur in this case, but rather the alternative electron hopping pathway. These results provide theoretical evidence that the two model peptides follow different electron transfer pathways, due to their different conformations with only peptide **2** possessing a well-defined secondary structure. For the first time, we have established a direct link between electron transfer dynamics and electron transfer kinetics for the two distinctive mechanisms (pathways) in peptides.

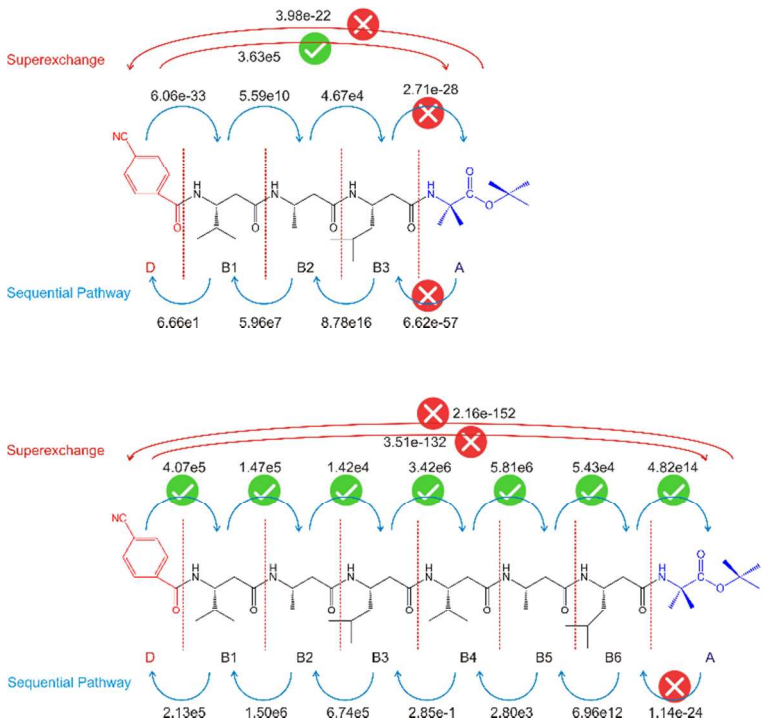

Figure 2. Constructed diabatic states for **1** (top) and **2** (bottom), and the two possible electron transfer pathways. Computed electron transfer rate constants (s^{-1}) for each step are labelled along each arrow. Symbols ⊗ and ✓ indicate an improbable and possible elementary electron transfer step respectively.

3. BACKBONE RIGIDITY AND CONTROLLABLE MECHANISTIC TRANSITION

Having established this link, we then designed a series of novel peptides that allow us to modulate the electron transfer kinetics, by altering the electron transfer dynamics through structural modification. This is of prime importance, as the functions of molecular electronic components, unlike in conventional electronics, are brought about by inducing changes in the molecular structure to provide desirable properties, such as multiple electronic states. We know that incorporation of a side-bridge constraint into a peptide increases backbone rigidity,[27] which may provide a level of control over electron transfer kinetics. The influence of these effects on electron transfer was defined by conducting electrochemical studies on synthetic helical peptides **3**-**8** (Figure 3), containing constrained species and their linear counterparts to provide prominent structural differences. Specifically, linear peptides **4**, **6** and **8** comprise triazole-, alkene- and amide-functionalized side-chains respectively. These same groups are found in the macrocyclic peptides **3**, **5** and **7**, the backbones of which are further constrained into a 3_{10}-helix with a side-bridge linking the *i* and *i*+3 residues (as shown in Figure 3). The component geminally disubstituted Aib (α-aminoisobutyric acid) residues of **3-8** promote formation of a common 3_{10}-helical geometry, as demonstrated by molecular modelling and spectroscopic characterization.[16,28,29] Thus, as these peptides each share a similar well-defined backbone geometry, any disparity in the electron transfer kinetics can be directly correlated to the associated dynamic effects arising from the presence (or absence) of the side-bridge constraint.

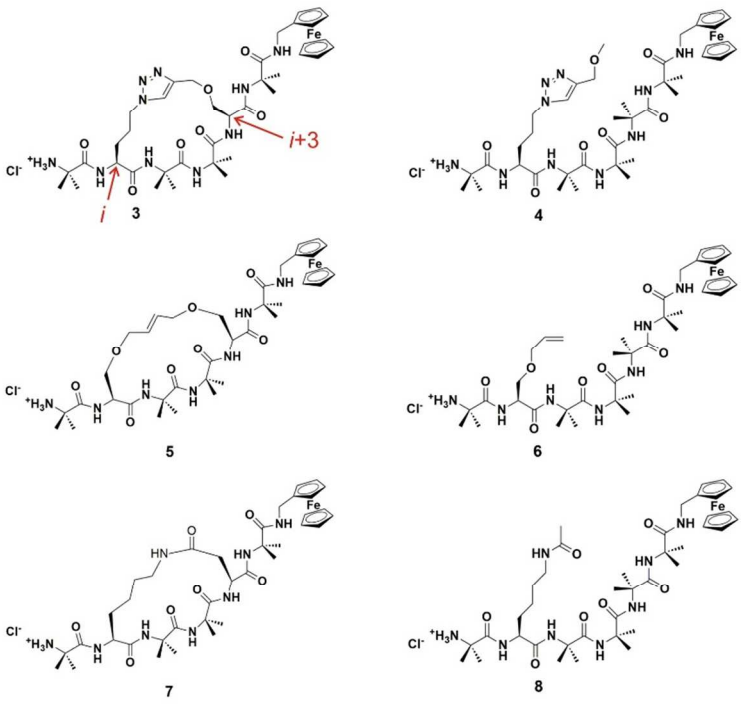

Figure 3. 3_{10}-helical peptides **3**-**8**.

Cyclic voltammograms for each peptide show a pair of redox peaks (Figure 4).[30] The constrained peptides (**3**, **5** and **7**) and their linear analogues (**4, 6** and **8**) exhibit considerably different formal potentials (E_o) and electron transfer rate constants (k_{ET}), and fall into two distinct groups. The linear analogues each display low E_o and high k_{ET} values, estimated to be 0.371 V and 117.3 s^{-1} for **4**,[28] 0.380 V and 260.4 s^{-1} for **6**,[29] 0.442 V and 83.7 s^{-1} for **8**.[16] Contrary to this, the constrained peptides exhibit high E_o and low k_{ET} values, estimated to be 0.853 V and 28.1 s^{-1} for **3**,[28] 0.844 V and 17.5 s^{-1} for **5**,[29] 0.924 V and 9.3 s^{-1} for **7**.[16] Each constrained peptide shows a significant formal potential shift to the positive, between 460 mV and 480 mV, in comparison to their linear counterparts. Such a dramatic formal potential shift in ferrocene-derivatized peptides has not been previously reported, with the magnitude of this shift significantly higher than other conformation-dependent structures

such as *cis-trans* cyclohexasilanes (110 mV),[31] placing it between the voltage drops across a germanium (300 mV-350 mV) and a silicon (600 mV-700 mV) p-n junction. The observed electron transfer rate constants for each constrained peptide are between four and 15-fold lower than that of their linear counterparts. We have previously found similar results in peptides comprising a β-strand conformation,[16,29,32] which confirms the commonality of these effects from a side-bridge constraint on electron transfer kinetics, irrespective of the type of secondary structure and/or the means of cyclization. Our theoretical data support the experimental results,[28] suggesting that side-bridge stapling creates an additional reorganization energy barrier that impedes electron transfer by restricting the precise torsional motions (dynamics) within the peptide, in turn decreasing the rate of charge transfer (kinetics). Thus, a side-bridge constraint provides a unique approach to manipulate energy barriers and hence electron transfer kinetics in peptides. These vast formal potential shifts and electron transfer rate constant drops provide two distinct electronic states with a sizeable differential (i.e. on/off), which is ideal for the design of molecular switches.

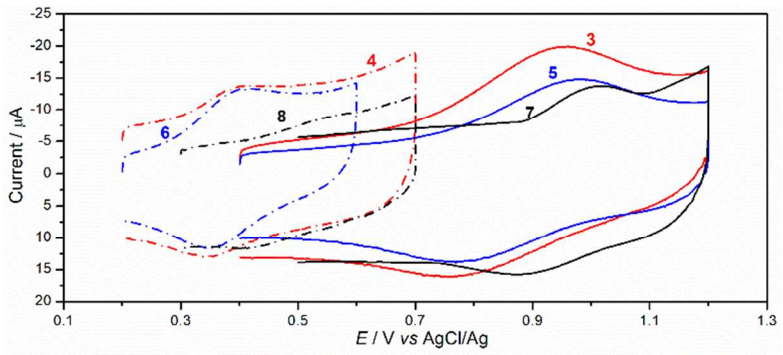

Figure 4. Cyclic voltammograms for constrained peptides **3** (red solid), **5** (blue solid), **7** (black solid), and their linear counterparts **4**, **6**, **8** (dashed lines in corresponding colors) taken at 5 V s^{-1} in 0.1 mol L^{-1} $TBAPF_6/CH_3CN$ solutions.

Having demonstrated that we can modulate the electron transfer kinetics in peptides by judicious structural modification, we set our sights on elucidating the mechanisms responsible for such transference, as this is an important step toward the design and fabrication of bio-inspired, next generation electronic components. Charge transfer in linear 3_{10}-helical peptides such as **4**, **6** and **8** is understood to proceed *via* a hopping mechanism,[1,17] however very little is known about electron transfer mechanistic pathways in constrained peptides. In light of this, Marcus theory in conjunction with cDFT is used to address this fundamental issue. The model peptides for this computational study (**9** and **10**, see Figure 5) are analogues of **7** and **8**, albeit with redox-active ferrocene units at both termini to act as electron donor and acceptor.[28,33] Three key charge transfer pathways are depicted in Figure 5. One particular pathway involves one-step superexchange between the first and last residues (Aib1 and Aib6, green arrows). The others are two-step sequential hopping pathways originating at Aib1, either passing through the peptide backbone (Aib4, red arrows) or the amide-containing side-bridge/side-chain (blue arrows), terminating at Aib6.

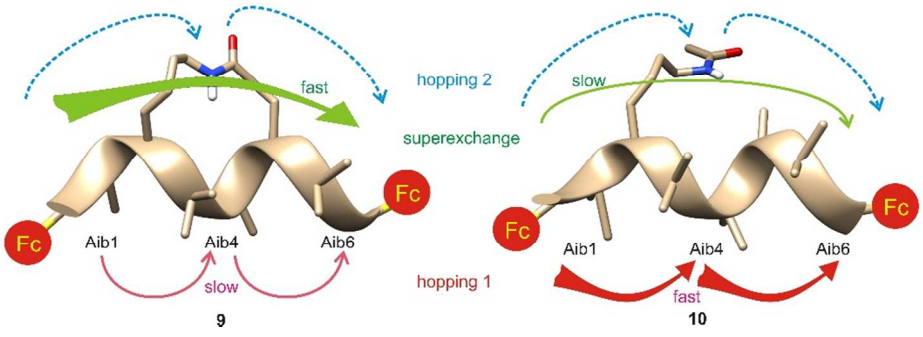

Figure 5. Constrained peptide **9** (left) and linear **10** (right), showing three key electron transfer pathways.

The overall computed superexchange electron transfer rate constant (k_{super}) is 2.28×10^{11} s^{-1} for the constrained peptide **9**, while the overall hopping electron transfer rate constant *via* its backbone is lower, $k_{hop1} = 2.36\times10^{9}$ s^{-1}. In contrast, the linear **10** has an overall k_{super} of 6.57×10^{12} s^{-1}, while the overall k_{hop1} via the backbone is greater (1.00×10^{15} s^{-1}). This shows that the superexchange pathway is the most favorable in the constrained **9**, while the hopping pathway via the backbone is favored in the linear **10**. For the first time, a clear transition from hopping to superexchange as a result of side-bridge gating is clearly demonstrated in two well-defined helical peptides, which progresses the fundamental knowledge gleaned from our earlier study, where only peptide **2** possesses a well-defined secondary structure and **1** is ill-defined. These data reinforce our experimental observations discussed earlier, where the linear peptides exhibit lower formal potentials and higher electron transfer rate constants, relative to their constrained counterparts. We believe that restricting the electron transfer dynamics in the helical peptide through the introduction of a side-bridge constraint, reduces the vibrational fluctuations in the backbone to such an extent that a hopping mechanism can no longer operate, which in turn lowers the electron transfer kinetics. We have also shown that both mechanisms can operate in a single peptide, for example $k_{super} = 2.28\times10^{11}$ s^{-1} and $k_{hop1} = 2.37\times10^{9}$ s^{-1} in **9**, with one favored over the other. Furthermore, the overall hopping electron transfer rate constants through the side-bridge of the constrained **9**, and the side-chain of the linear **10**, are exceptionally low (1.96×10^{-38} s^{-1} for **9**, and 4.38×10^{-41} s^{-1} for **10**), ruling out any possibility of hopping through these pathways. These discoveries not only add considerable weight to the notion that electron transfer utilizes both the superexchange and hopping mechanisms,[26,34] they also challenge the widely accepted hypothesis that the mechanisms responsible for electron transfer in peptides are solely distance-dependent. This

is indicative of how nature has evolved rather subtle and ingenious methods to regulate electron transfer by protein dynamics in complexes such as cytochrome bc_1, and conformational gating in cytochrome cd_1[35] and nitrogenase.[36] These findings unveil a new pragmatic approach for controlling the mechanisms responsible for charge transfer in helical peptides through the introduction of a side-bridge, which is strategic to the design of stable building blocks for future three-dimensional peptide-based circuitry.

4. ELECTRON RICH SIDE-CHAINS AS 'STEPPING STONES'

With the success of finding two distinct electronic states, i.e. on/off, in the linear and constrained species, our next study set out to fine-tune the electronic properties of peptides. Structural modification is once again achieved through the inclusion of appropriate side-bridge constraints, while we introduce a number of electron-rich side-chains into the peptides to determine their effects on electron transfer kinetics. In particular, a series of alkene containing peptides (linear **6**, **12**, **13**, **14** and constrained **5** and **11**, see Figures 3 and 6) is used to unravel the interplay of peptide backbone rigidity (dynamics) and the nature of the amino acid side chains, where previously these effects have been considered without factoring in the other variable. A combination of ^{1}H NMR, IR, and molecular modelling, demonstrate that all these peptides share a remarkably similar 3_{10}-helical conformation.[29]

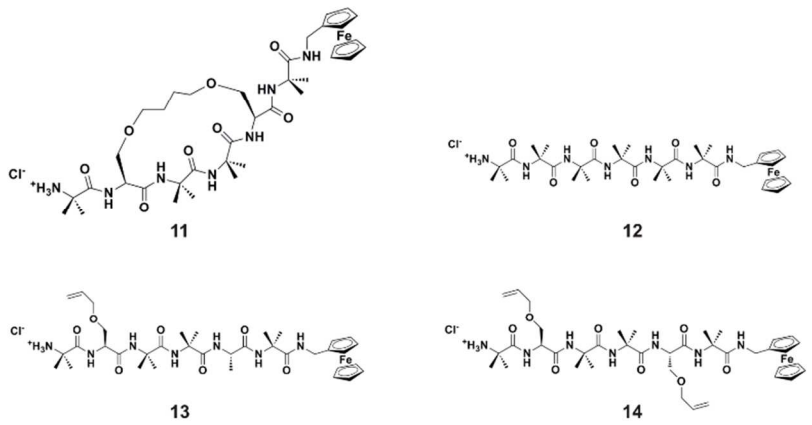

Figure 6. 3_{10}-helical peptides **11-14**.

Cyclic voltammograms for each of these helical peptides are shown in Figure 7. A comparison of the electrochemical data for peptides **5**, **6** and **13** provide some insight into the influence of backbone rigidity, where these peptides share a common 3_{10}-helical geometry and the presence of a single electron-rich alkene. Peptide **5** is constrained and hence rigidified by its tether. Peptide **6** contains five Aib residues, while peptide **13** would be the most flexible of the three, as one Aib residue is replaced by an alanine. The electrochemical data reveals a k_{ET} value of 17 s^{-1} for the constrained **5**, a clear 15-20 fold lower than those of the linear **6** and **13**. Peptide **6** gives the next lowest k_{ET} (260 s^{-1}), with the most flexible peptide **13** (307 s^{-1}). These results clearly support the notion that increased backbone rigidity impedes electron transfer kinetics by restricting the precise torsional motion required for a hopping mechanism. A comparison of the data for the three linear peptides (**6**, **12**, and **14**) provides a measure of the influence of the electron-rich alkene side-chains on the rate of electron transfer, somewhat in isolation from the effects of backbone rigidity. Peptide **14**, with alkenes at both the *i* and *i*+3 positions, exhibits the largest k_{ET} of 388 s^{-1}. Peptide **6** containing one alkene side-chain gives a k_{ET} of 260 s^{-1}, while peptide **12**, which lacks an alkene side-chain in its sequence, gives a

much reduced k_{ET} of 62 s^{-1}. The electron transfer rate constant clearly increases with the increasing number of electron-rich alkenes in the peptides, which presumably facilitate electron transfer by way of a hopping mechanism utilizing the alkenes as 'stepping stones'. However, the relative rigidity of the backbones of peptides **6**, **12**, and **14** may also contribute to the rate of electron transfer, which would be expected to decrease with increasing numbers of Aib units through the series.[28] A comparison of the data for **13** and **14** sheds further light on this. These two peptides contain the same number of Aib units and differ only in the number of alkenyl groups to act as potential 'stepping stones'. The observed k_{ET} for **14** is 388 s^{-1}, 20% higher than that of **13** (307 s^{-1}), clearly demonstrating the ability of the alkene groups to facilitate electron transfer through the peptide by acting as a 'stepping stone'.

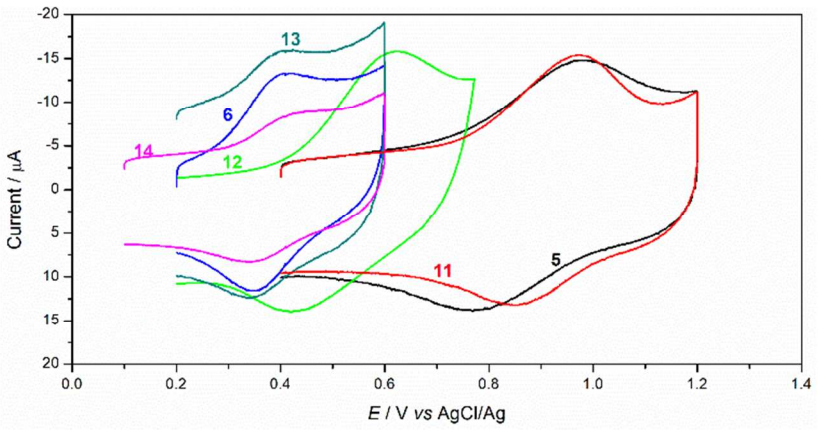

Figure 7. Cyclic voltammograms for 3_{10}-helical peptides **5**, **6** and **11-14** taken at 5 V s^{-1} in 0.1 mol L^{-1} $TBAPF_6/CH_3CN$ solutions.

A Löwdin electron population analysis was conducted to provide information on partial charge distribution in the Aib and modified serine with terminal alkene (Table 1), as these residues are

contained in the linear peptides. Approximately 88% of the extra charge is distributed on the amide region when the positive charge (+1) is injected into the Aib residue. This emphasizes the significant contribution made by the amide region to intramolecular electron transfer through the peptide backbone, clearly demonstrating the participation of a through-bond hopping mechanism.[21] However, only 68% of the extra charge is distributed on the amide region, with the electron-rich alkene side-chain holding approximately 20% of the extra charge localized on the residue, when the positive charge (+1) is injected into the modified serine residue. This further confirms the role of the electron-rich alkene side-chain as a 'stepping stone' for electron transfer. These findings offer a new approach to fine tune the electronic properties of peptides *via* structural modifications to the backbone to increase/decrease rigidity, and chemical modifications through the inclusion of electron-rich side-chains. Such peptides with diverse and tunable electronic functions, open new avenues for the design of future bio-inspired molecular electronic devices.

Table 1. Löwdin charge distribution analysis of uncharged and charged amino acid residues Aib, and modified serine with terminal alkene.

	Aib	modified serine
Löwdin analysis of uncharged residue	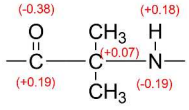	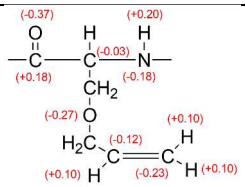
Löwdin analysis with an overall charge of +1	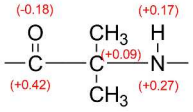	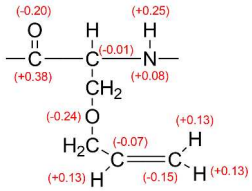
Charge localized on amide region	0.88	0.68
Charge localized on		0.22

$CH=CH_2$ (alkene)

5. INTERPLAY OF BACKBONE RIGIDITY AND QUANTUM INTERFERENCE ON ELECTRONIC TRANSPORT

Our earlier studies demonstrated that the additional backbone rigidity, imparted by a side-bridge constraint, restricts the vibrational fluctuations (torsional motion) necessary for facile electron transfer through the backbone of the peptide.[30,32,37] However, the side-bridge constraint may also provide an additional electron transfer pathway, analogous to a parallel circuit. As demonstrated in Figure 8a (top) on reaching the first juncture, the electron wave traversing the backbone from sections M0 to M2 would split into two individual waves, propagating along the backbone (M1) and side-bridge (M3) respectively. They re-emerge at the second juncture and superimpose to form a resultant wave, eventually passing through the backbone (section M2). This wave will have either greater or lower amplitude than the original (i.e. the effects of quantum interference[38]) if the two individual waves differ in amplitude and phase arising from the different structural and chemical compositions of sections M1 and M3. With this in mind, we set out to determine if a side-bridge constraint can influence electronic transport by providing an alternative pathway, hence revealing the effects of quantum interference; or simply increase the backbone rigidity of the peptide to impede such transport. Peptides **15** and **17** (Figure 8) are constrained into well-defined β-strand and 3_{10}-helical conformations respectively with an amide-containing side-bridge, while peptides **16** and **18** are direct linear analogues. These peptides were purposely chosen, as many proteins have evolved specifically for electron transfer[15] by utilizing a sophisticated framework, provided by well-defined secondary structures including helices and β-sheets.

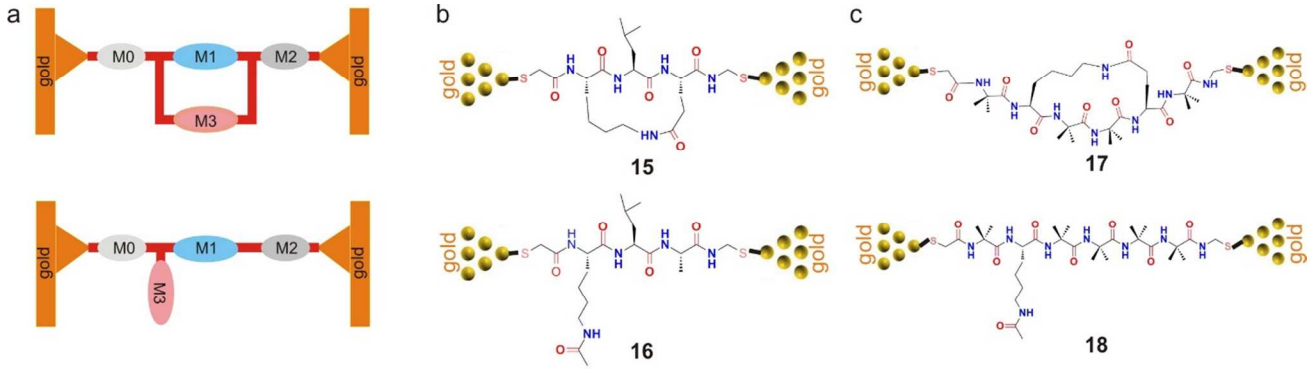

Figure 8. (a) Single-peptide circuits containing constrained/parallel (top) and linear/simple (bottom) pathways. (b**)** Molecular junctions comprising β-strand constrained **15** and linear **16**. (c) Molecular junctions comprising 3_{10}-helical constrained **17** and linear **18**.

Initially, transmission spectra for the β-strand peptides were calculated using the NEGF-DFT approach.[39] As shown in Figure 9a, the transmission coefficient of the constrained **15** (red curve) is lower than that of the linear **16** (blue curve) at most energies. Notably, the constrained **15** exhibits one strong negative dip in transmission close to the Fermi energy, with the transmission coefficient exceeding 1E-13 near 0.85 eV (Figure 9a, black highlighted region). This feature is considered the opposite of a transmission resonance, namely an anti-resonance,[40] which is known to be a direct result of destructive quantum interference.[38,41] The appearance of anti-resonance is a definitive consequence of the divergent charge transport pathways in the constrained peptide, that differ both spatially and energetically.[42] This is further evidenced in the eigenchannels of peptide **15** (Figure 9b), which are especially useful for interpreting the contributions from particular molecular orbitals (energies) for electronic transport through the molecular junction.[43] The eigenchannels of **15** exhibit a discontinuous distribution of the wavefunction density along both the backbone and side-bridge (Figure 9b, top). In contrast, computed eigenchannels for the linear **16** span the entire pathway,

exhibiting a continuous electron waveform along the backbone represented by the alternating purple and light blue regions (Figure 9b, bottom). Conductance values for the constrained **15** and linear **16** were calculated to be 1.1 $\times 10^{-11}$ S and 2.3 $\times$ 10^{-10} S respectively. These results correlate with our corresponding electrochemical study,[16] where the electron transfer rate constant for the analogous constrained peptide (5.92 s^{-1}) was also found to be more than one order of magnitude lower than that of its linear analogue (86.67 s^{-1}). We previously found a similar correlation for constrained/linear β-strand peptides comprising a triazole side-bridge.[32] Despite peptides **15** and **16** sharing a common β-strand conformation, the effects of destructive quantum interference are found to occur essentially in the constrained peptide, through the heterogenous backbone and the additional tunnelling pathway provided by the side-bridge constraint, which represents a distinct form of quantum interferometer.

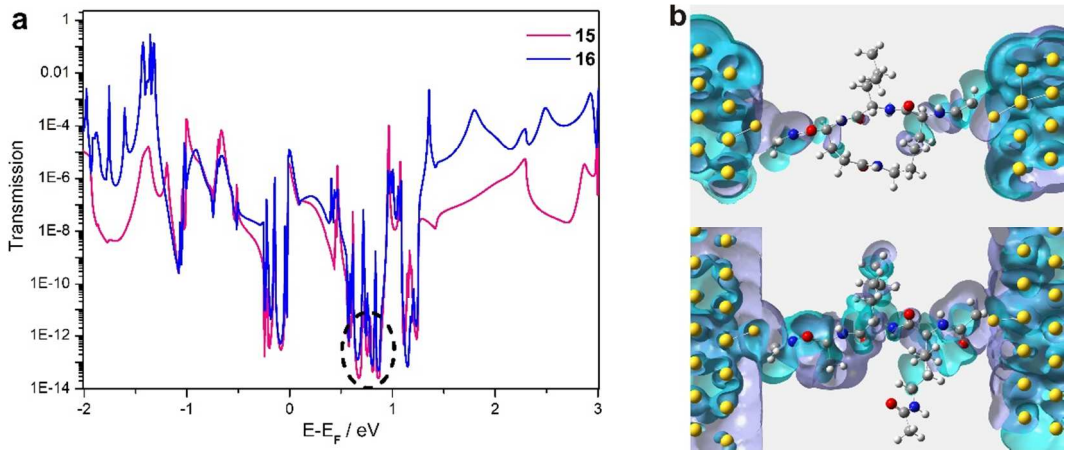

Figure 9. (a) Transmission spectra for the parallel (constrained β-strand **15**, red) and simple (linear β-strand **16**, blue) circuits at a bias voltage of 0 V. (b) Eigenchannels for the constrained (**15**, top) and linear (**16**, bottom) circuits at E-E_F=0 eV.

Contrary to the results from the β-strand peptides, transmission spectra for the 3_{10}-helical **17** and **18** (analogues of **7** and **8**, see Figure 3) exhibit four strong dips close to the Fermi energy, with the transmission coefficient exceeding 1E-16 at 0.85 eV (Figure 10a). The presence of multiple anti-resonance peaks[42] in both molecular junctions indicates multi-tunnelling electronic transport pathways in these helical peptides. The destructive quantum interference effects are further confirmed by the discontinuous distribution of wavefunction density in the eigenchannels of both peptides (Figure 10b). Notably, the computed conductance values for the constrained and linear helical peptides are remarkably similar, 3.1×10^{-14} S and 3.2×10^{-14} S respectively. However, the electron transfer rate constant observed for the constrained analogue **7** (9.34 s^{-1}) is approximately one order of magnitude lower than that of the linear **8** (83.65 s^{-1}). No such correlation is found between the computed conductance values and the observed electron transfer rate constants in these helical peptides (**7** and **8**; **17** and **18**), which contrasts data from the β-strand peptides.

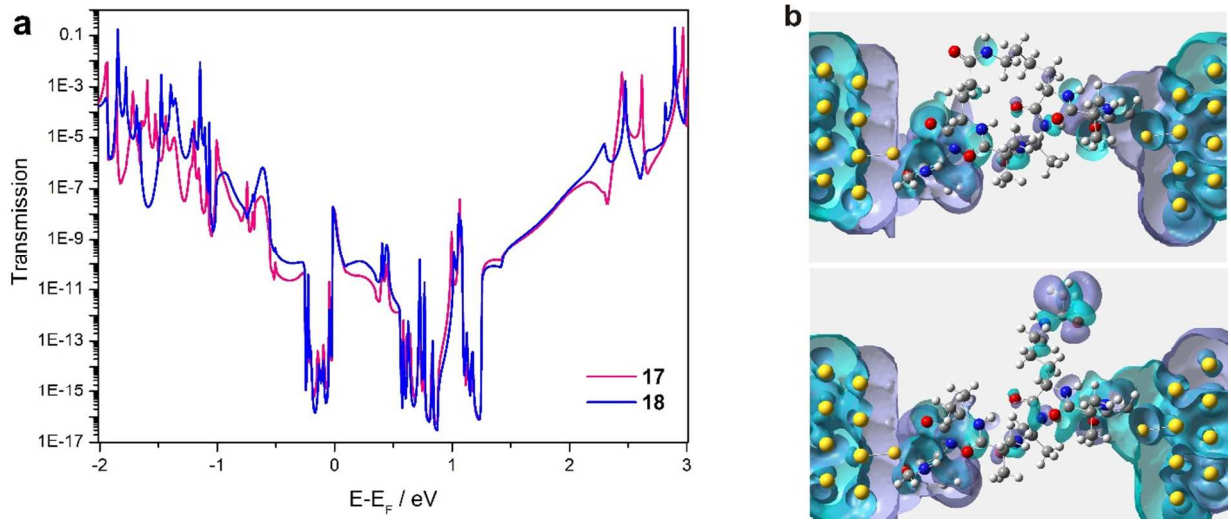

Figure 10. (a) Transmission spectra for the parallel (constrained 3_{10}-helical **17**, red) and simple (linear 3_{10}-helical **18**, blue) circuits at a bias voltage of 0 V. (b) Eigenchannels for the constrained (**17**, top) and linear (**18**, bottom) circuits at $E-E_F=0$ eV.

Although the elastic transport simulations for the linear helical **18** (analogue of **8**) demonstrate the existence of destructive quantum interference effects, the vibrational fluctuations along the flexible backbone lead to a quenching of these effects at room temperature, which is reflected by the higher k_{ET} (83.65 s^{-1}). Our computational study shows that the additional energy barrier (0.14 eV - 0.30 eV)[16] brought about by the side-bridge constraint restricts such vibrational fluctuations, which is reflected by a lower k_{ET} (9.34 s^{-1}). Hence quantum interference effects come to the fore, as demonstrated by the anti-resonance peaks (Figure 10). These findings provide direct evidence of interplay between destructive quantum interference effects and vibrational fluctuations, as both phenomena contribute to charge transfer to varying degrees, depending on the extent of backbone rigidity. We have thus demonstrated another unique form of peptide-based quantum interferometer, where the effects of destructive quantum interference are enhanced by increasing backbone rigidity through the introduction of a side-bridge constraint, while reducing vibrational fluctuations required by a hopping mechanism. Hence, these exciting findings offer a new approach to control electronic transport in peptides through the modulation of electron wavefunctions and backbone rigidity, which paves the way for the design of interference-controlled components, with applications in areas such as biosensing, quantum information processing, and thermoelectrics.

6. SUMMARY AND OUTLOOK

Bio-inspired molecular electronics offers a greener approach to progress existing fields such as conventional electronics, energy conversion, and sensing technologies. We have summarized our recent key findings and contributions to this rapidly expanding field of research, with wide

implications to future fabrication of advanced peptide-based devices. We present both electrochemical and first principles studies as follows: (1) The study of β-peptides **1** and **2** clearly shows that the electron transfer mechanism is defined by the extent of secondary structure, rather than simply peptide chain length. The first principles approach corroborates experimental observations, which establishes a link between electron transfer dynamics and kinetics in peptides. (2) Electrochemical studies reveal that constrained peptides exhibit a significant formal potential shift to the positive and a substantial decrease in the electron transfer rate constant, compared to their linear counterparts. These vast disparities afford a sizeable differential, which is ideal for the design of molecular switches. Furthermore, high level calculations reveal for the first time a clear transition from hopping to superexchange as a result of side-bridge gating. (3) Experimental results on a series of alkene-containing peptides unravel an interplay between peptide backbone rigidity and the nature of the amino acid side chains, in defining the electron transfer kinetics. Electron population analysis provides the first clear theoretical evidence that amide groups act as hopping sites, and confirms the role of alkene side-chains as 'stepping stones' for electron transfer. (4) Electronic transport simulations reveal two distinct forms of peptide-based quantum interferometers. The effects of destructive quantum interference in the constrained β-strand peptide occur essentially through the backbone and the additional tunnelling pathway provided by the side-bridge, whereas an interplay between destructive quantum interference effects and vibrational fluctuations is revealed in the helical peptides. Collectively, these important fundamental advances bring us a step closer to realizing our ultimate goal to design, assemble and control functional devices from the bottom up.

AUTHOR INFORMATION

Corresponding Authors

*e-mail: jingxian.yu@adelaide.edu.au.

*e-mail: andrew.abell@adelaide.edu.au.

Funding Sources

We acknowledge the Australian Research Council (ARC) for the financial support of this work.

Notes

The authors declare no competing financial interest.

Biographies

Jingxian Yu received his PhD at Flinders University in 2009. He joined the University of Adelaide as an ARC Australian Postdoctoral Fellow later that year. He is currently a senior research fellow working on electron transfer in peptides.

John R Horsley received his PhD at the University of Adelaide in 2015, where he is currently working as a Postdoctoral Fellow in the area of electron transfer in peptides.

Andrew D Abell received his PhD at the University of Adelaide, where he is currently Professor of Chemistry and Adelaide Node Director of the Centre for Nanoscale BioPhotonics (CNBP).

REFERENCES

(1) Arikuma, Y.; Nakayama, H.; Morita, T.; Kimura, S. Electron Hopping over 100 angstrom Along an alpha Helix. *Angewandte Chemie-International Edition* **2010**, *49*, 1800.

(2) Amdursky, N.; Marchak, D.; Sepunaru, L.; Pecht, I.; Sheves, M.; Cahen, D. Electronic Transport via Proteins. *Advanced Materials* **2014**, *26*, 7142-7161.

(3) Lerner Yardeni, J.; Amit, M.; Ashkenasy, G.; Ashkenasy, N. Sequence dependent proton conduction in self-assembled peptide nanostructures. *Nanoscale* **2016**, *8*, 2358-2366.

(4) Kracht, S.; Messerer, M.; Lang, M.; Eckhardt, S.; Lauz, M.; Grobety, B.; Fromm, K. M.; Giese, B. Electron Transfer in Peptides: On the Formation of Silver Nanoparticles. *Angewandte Chemie-International Edition* **2015**, *54*, 2912-2916.

(5) Maruccio, G. Molecular electronics: Protein transistors strike gold. *Nature Nanotechnology* **2012**, *7*, 147-148.

(6) Wardrip, A. G.; Mazaheripour, A.; Husken, N.; Jocson, J. M.; Bartlett, A.; Lopez, R. C.; Frey, N.; Markegard, C. B.; Kladnik, G.; Cossaro, A.; Floreano, L.; Verdini, A.; Burke, A. M.; Dickson, M. N.; Kymissis, I.; Cvetko, D.; Morgante, A.; Sharifzadeh, S.; Nguyen, H. D.; Gorodetsky, A. A. Length-Independent Charge Transport in Chimeric Molecular Wires. *Angewandte Chemie-International Edition* **2016**, *55*, 14265-14269.

(7) Xiao, X. Y.; Xu, B. Q.; Tao, N. J. Conductance titration of single-peptide molecules. *Journal of the American Chemical Society* **2004**, *126*, 5370-5371.

(8) Uji, H.; Morita, T.; Kimura, S. Molecular direction dependence of single-molecule conductance of a helical peptide in molecular junction. *Phys. Chem. Chem. Phys.* **2013**, *15*, 757-760.

(9) Scullion, L.; Doneux, T.; Bouffier, L.; Fernig, D. G.; Higgins, S. J.; Bethell, D.; Nichols, R. J. Large Conductance Changes in Peptide Single Molecule Junctions Controlled by pH. *Journal of Physical Chemistry C* **2011**, *115*, 8361-8368.

(10) Baghbanzadeh, M.; Bowers, C. M.; Rappoport, D.; Zaba, T.; Gonidec, M.; Al-Sayah, M. H.; Cyganik, P.; Aspuru-Guzik, A.; Whitesides, G. M. Charge Tunneling along Short Oligoglycine Chains. *Angewandte Chemie-International Edition* **2015**, *54*, 14743-14747.

(11) Sek, S. Review peptides and proteins wired into the electrical circuits: An SPM-based approach. *Biopolymers* **2013**, *100*, 71-81.

(12) Malak, R. A.; Gao, Z. N.; Wishart, J. F.; Isied, S. S. Long-range electron transfer across peptide bridges: The transition from electron superexchange to hopping. *Journal of the American Chemical Society* **2004**, *126*, 13888.

(13) Cordes, M.; Giese, B. Electron transfer in peptides and proteins. *Chemical Society Reviews* **2009**, *38*, 892-901.

(14) Antonello, S.; Maran, F. Intramolecular dissociative electron transfer. *Chemical Society Reviews* **2005**, *34*, 418.

(15) Shah, A.; Adhikari, B.; Martic, S.; Munir, A.; Shahzad, S.; Ahmad, K.; Kraatz, H. B. Electron transfer in peptides. *Chemical Society Reviews* **2015**, *44*, 1015-1027.

(16) Yu, J.; Horsley, J. R.; Abell, A. D. Exploiting the interplay of quantum interference and backbone rigidity on electronic transport in peptides: a step towards bio-inspired quantum interferometers. *Molecular Systems Design & Engineering* **2017**, *2*, 67-77.

(17) Yu, J.; Zvarec, O.; Huang, D. M.; Bissett, M. A.; Scanlon, D. B.; Shapter, J. G.; Abell, A. D. Electron Transfer through α-Peptides Attached to Vertically Aligned Carbon Nanotube Arrays: A Mechanistic Transition. *Chemical Communications* **2012**, *48*, 1132–1134.

(18) Wenger, O. S. How Donor−Bridge−Acceptor Energetics Influence Electron Tunneling Dynamics and Their Distance Dependences. *Accounts of Chemical Research* **2011**, *44*, 25.

(19) Amdursky, N. Electron Transfer across Helical Peptides. *Chempluschem* **2015**, *80*, 1075-1095.

(20) Bostick, C. D.; Mukhopadhyay, S.; Pecht, I.; Sheves, M.; Cahen, D.; Lederman, D. Protein bioelectronics: a review of what we do and do not know. *Reports on Progress in Physics* **2018**, *81*.

(21) Yu, J.; Huang, D. M.; Shapter, J. G.; Abell, A. D. Electrochemical and Computational Studies on Intramolecular Dissociative Electron Transfer in beta-Peptides. *Journal of Physical Chemistry C* **2012**, *116*, 26608-26617.

(22) Goodman, C. M.; Choi, S.; Shandler, S.; DeGrado, W. F. Foldamers as versatile frameworks for the design and evolution of function. *Nature Chemical Biology* **2007**, *3*, 252-262.

(23) Seebach, D.; Gardiner, J. beta-Peptidic Peptidomimetics. *Accounts of Chemical Research* **2008**, *41*, 1366-1375.

(24) Yu, J.; Horsley, J. R.; Abell, A. D. The Influence of Secondary Structure on Electron Transfer in Peptides. *Australian Journal of Chemistry* **2013**, *66*, 848-851.

(25) Marcus, R. A.; Sutin, N. Electron transfers in chemistry and biology. *Biochimica Et Biophysica Acta* **1985**, *811*, 265-322.

(26) Petrov, E. G.; Shevchenko, Y. V.; May, V. On the length dependence of bridge-mediated electron transfer reactions. *Chemical Physics* **2003**, *288*, 269-279.

(27) Jacobsen, O.; Maekawa, H.; Ge, N. H.; Gorbitz, C. H.; Rongved, P.; Ottersen, O. P.; Amiry-Moghaddam, M.; Klaveness, J. Stapling of a 3(10)-Helix with Click Chemistry. *Journal of Organic Chemistry* **2011**, *76*, 1228.

(28) Yu, J.; Horsley, J. R.; Moore, K. E.; Shapter, J. G.; Abell, A. D. The Effect of a Macrocyclic Constraint on Electron Transfer in Helical Peptides: A Step Towards Tunable Molecular Wires *Chemical Communications* **2014**, *50*, 1652.

(29) Horsley, J. R.; Yu, J.; Moore, K. E.; Shapter, J. G.; Abell, A. D. Unraveling the Interplay of Backbone Rigidity and Electron Rich Side-Chains on Electron Transfer in Peptides: The Realization of Tunable Molecular Wires. *Journal of the American Chemical Society* **2014**, *136*, 12479-12488.

(30) Yu, J.; Horsley, J. R.; Abell, A. D. Turning electron transfer 'on-off' in peptides through side-bridge gating. *Electrochimica Acta* **2016**, *209*, 65-74.

(31) Emanuelsson, R.; Löfås, H.; Wallner, A.; Nauroozi, D.; Baumgartner, J.; Marschner, C.; Ahuja, R.; Ott, S.; Grigoriev, A.; Ottosson, H. Configuration- and Conformation-Dependent Electronic-Structure Variations in 1,4-Disubstituted Cyclohexanes Enabled by a Carbon-to-Silicon Exchange. *Chemistry – A European Journal* **2014**, *20*, 9304-9311.

(32) Horsley, J. R.; Yu, J.; Abell, A. D. The Correlation of Electrochemical Measurements and Molecular Junction Conductance Simulations in beta-Strand Peptides. *Chemistry-A European Journal* **2015**, *21*, 5926-5933.

(33) Ding, F. Z.; Wang, H. B.; Wu, Q.; Van Voorhis, T.; Chen, S. W.; Konopelski, J. P. Computational Study of Bridge-Assisted Intervalence Electron Transfer. *Journal of Physical Chemistry A* **2010**, *114*, 6039-6046.

(34) Lambert, C.; Noll, G.; Schelter, J. Bridge-mediated hopping or superexchange electron-transfer processes in bis(triarylamine) systems. *Nature Materials* **2002**, *1*, 69-73.

(35) Sharp, R. E.; Chapman, S. K. Mechanisms for regulating electron transfer in multi-centre redox proteins. *Biochimica Et Biophysica Acta-Protein Structure and Molecular Enzymology* **1999**, *1432*, 143-158.

(36) Danyal, K.; Mayweather, D.; Dean, D. R.; Seefeldt, L. C.; Hoffman, B. M. Conformational Gating of Electron Transfer from the Nitrogenase Fe Protein to MoFe Protein. *Journal of the American Chemical Society* **2010**, *132*, 6894-+.

(37) Schlag, E. W.; Sheu, S. Y.; Yang, D. Y.; Selzle, H. L.; Lin, S. H. Distal charge transport in peptides. *Angewandte Chemie-International Edition* **2007**, *46*, 3196-3210.

(38) Lambert, C. J. Basic concepts of quantum interference and electron transport in single-molecule electronics. *Chemical Society Reviews* **2015**, 875-888.

(39) Brandbyge, M.; Mozos, J. L.; Ordejon, P.; Taylor, J.; Stokbro, K. Density-functional method for nonequilibrium electron transport. *Physical Review B (Condensed Matter and Materials Physics)* **2002**, *65*, 165401/165401-165417.

(40) Guedon, C. M.; Valkenier, H.; Markussen, T.; Thygesen, K. S.; Hummelen, J. C.; van der Molen, S. J. Observation of quantum interference in molecular charge transport. *Nature Nanotechnology* **2012**, *7*, 304-308.

(41) Manrique, D. Z.; Huang, C.; Baghernejad, M.; Zhao, X.; Al-Owaedi, O. A.; Sadeghi, H.; Kaliginedi, V.; Hong, W.; Gulcur, M.; Wandlowski, T.; Bryce, M. R.; Lambert, C. J. A quantum circuit rule for interference effects in single-molecule electrical junctions. *Nature Communications* **2015**, *6*, 6389-6389.

(42) Solomon, G. C.; Andrews, D. Q.; Goldsmith, R. H.; Hansen, T.; Wasielewski, M. R.; Van Duyne, R. P.; Ratner, M. A. Quantum Interference in Acyclic Systems: Conductance of Cross-Conjugated Molecules. *Journal of the American Chemical Society* **2008**, *130*, 17301-17308.

(43) Paulsson, M.; Brandbyge, M. Transmission eigenchannels from nonequilibrium Green's functions. *Physical Review B* **2007**, *76*, 15117.